Component-level Performance and Mass Sensitivity Analysis of NEP MW-class Power System

Christopher Harnack[1], William Machemer[2], Dennis Nikitaev[3], Matthew Duchek[4]

Advanced Projects Denver, Analytical Mechanics Associates, Denver, CO, 80211

Nuclear electric propulsion (NEP) is a promising option towards enabling missions to Mars and is an area of interest for NASA's Space Nuclear Propulsion project. This project is currently investigating technology development opportunities for an NEP vehicle. Physics-based modeling can be used in the early stages of technology development to gain understanding of the effects of technology and performance assumptions on the system performance and mass. This information can then inform technology maturation planning for near term development. By using a Brayton power conversion model and vehicle mass model for megawatt class NEP applications, a sensitivity analysis is performed to assess the impact of individual components' performance on the power conversion system performance and system mass. A Monte Carlo simulation is also used to determine the variability in system mass based on uncertainty within the modeling parameters. The sensitivity analysis shows a high sensitivity to power conversion inlet temperature, compressor inlet temperature, and recuperator performance. A Monte Carlo analysis suggests a range of -10% to +15% for a 90% confidence interval on system mass based on the uncertainties in the model inputs.

I. Introduction

A nuclear electric propulsion (NEP) system coupled with a chemical propulsion stage in a hybrid vehicle is one propulsion alternative being developed by NASA for crewed Mars missions. [1] The key metrics defining the performance of such a system are the power of the system, which directly relates to the thrust of the electric propulsion system, and the power system specific mass, α_{PS}, measured in kg/kW$_e$. Given the early stage of development of a MW$_e$-class NEP system applicable to a crewed Mars mission, there is significant uncertainty in the α_{PS} that can be achieved in such a system. To inform technology development, a suite of system-level performance and mass models have been created and used to estimate the α_{PS} of a developed system. The sensitivity of the mass to various assumptions and inputs is examined and some uncertainties are quantified through Monte Carlo analysis over reasonable ranges of the input values. This examination of uncertainty can give technology development planners insight into which parameters are most significant in determining the mass of the power system. This view of uncertain results can give a more realistic picture than any single point design, and can be useful when setting key performance parameters (KPPs) for development as in Ref. [2].

The NEP system consists of the five Critical Technology Elements (CTEs) shown in Figure 1: the reactor and coolant subsystem (RXS), power conversion subsystem (PCS), power management & distribution subsystem (PMAD), electric propulsion subsystem (EPS), and primary heat rejection subsystem (PHRS). Of these, all but the EPS are included in the power system and the calculation of α_{PS}. The mass per unit power of the EPS is also a factor to consider and it is modeled separately for inclusion in the mission analysis described in Ref. [2].

[1] Aerospace Systems Engineer, Advanced Projects, AIAA Member
[2] Aerospace Systems Engineer, Advanced Projects, AIAA Member
[3] Aerospace Systems Engineer, Advanced Projects, AIAA Member
[4] Aerospace Engineering Manager, Advanced Projects, AIAA Member

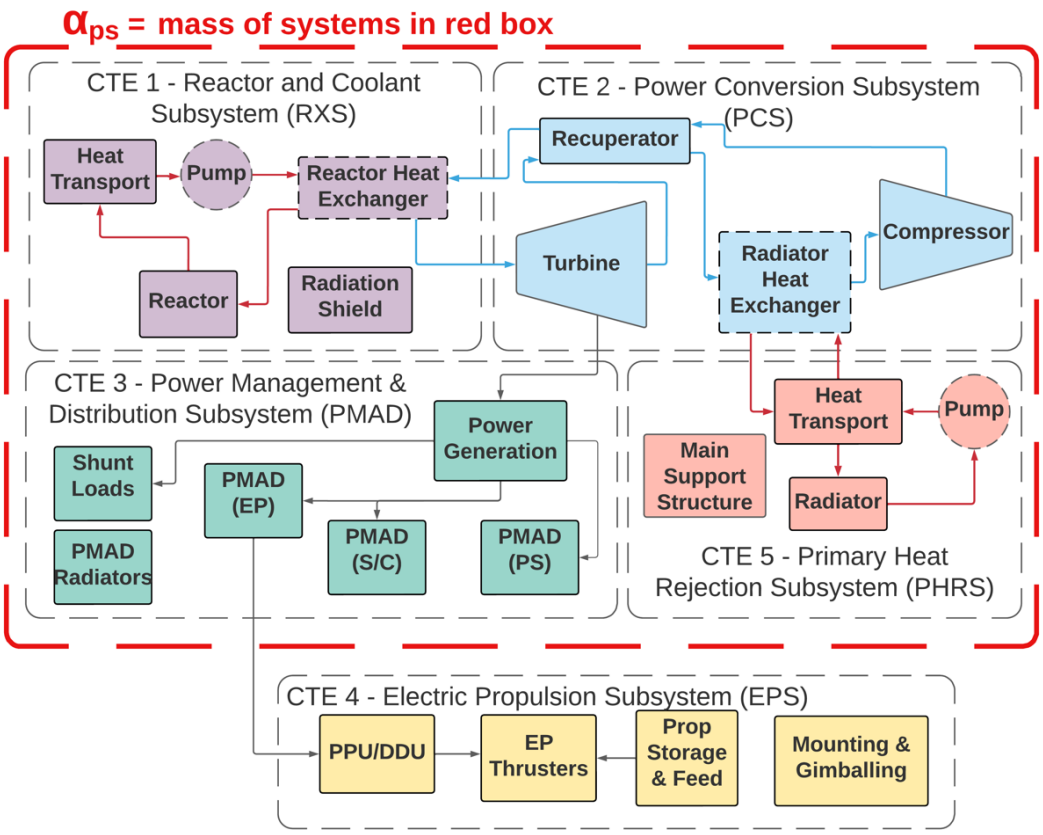

Figure 1. Critical technology elements (CTEs)

II. Description of Models

A. Performance Model

The performance model is numerically implemented in MATLAB/Simulink, solving for a closed steady-state thermodynamic power conversion cycle. The model outputs include component inlet and outlet states, component power, radiator area, and cycle efficiency. The model is based on the Brayton cycle and solves for the power flow through the following components: reactor, radiator, turbine, compressor, recuperator, alternator, and heat exchangers to the radiator and reactor subsystems, depending on the configuration. For the results in this paper, the cycle configuration chosen includes two fluid loops:

1. The Brayton fluid loop where the Brayton working fluid passes through the gas-cooled reactor and
2. The radiator loop which flows through a radiator, pump, and interfaces with the Brayton fluid loop at the radiator heat exchanger

A diagram of this power conversion system configuration is shown in Figure 2. The same models, with component modifications, have also been used to examine heat-pipe cooled and pumped liquid metal cooled reactor configurations.

The Brayton cycle uses He-Xe as the working fluid and the radiator loop uses eutectic NaK-78, based on recommendations from Ref. [3]. Specifics of the component design and modeling process are described in Ref. [4]. The enthalpy of the fluid was used for a majority of the thermodynamic process equations rather than employing a constant specific heat assumption. The model and optimization tolerances are chosen to balance model convergence time and reducing numerical error to less than 1%. Assumptions for the model were chosen based on literature and subject matter expert review. [5],[2]-[6] Due to the complexities of the reactor component, trendlines were developed for the pressure drop within the reactor core as a function of fluid inlet conditions. This is an improvement to the reactor model described previously in Ref. [4]. Results of the converged performance model are passed to the mass model to determine the α_{PS} for that system.

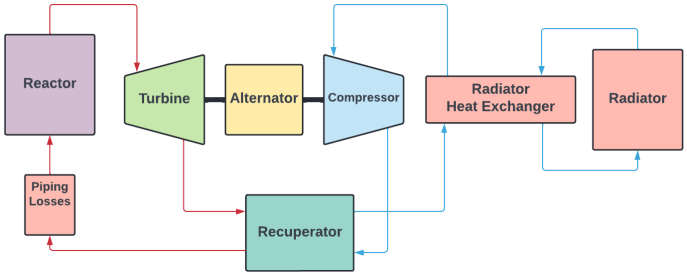

Figure 2. Diagram of performance model

A.1. Optimization Process

Specific technology performance assumptions for a given model configuration are input to the performance model which converges to a steady state thermodynamic cycle solution. Given a goal, such as the minimization of α_{PS}, the inputs can be adjusted to optimize for that goal. A subset of the possible Brayton input variables were varied in the optimization process based on their known influence on the resulting α_{PS} and on the capabilities and limits of the individual component mass models. Shown in Table 1 are the ranges and limits of the input variables that were used in the optimization process. A sweep of each variable and calculation of the α_{PS} resulting from that sweep was also performed to observe the general trends, with the result indicating that the local minima is also the global minima and that the results are smooth and well-behaved in this region.

Table 1. Variables considered in the optimization process

Input Variables	Reference Values	Value Limits	Limitation Reason
Turbine inlet pressure (Pa)	Optimized	2.1 - 4.8 MPa	Lower limit allows for reasonable reactor core pressure drop
Compressor inlet temperature (K)	Optimized	330K - 490K	Lower limit prevents phase change of fluids
Turbine PR	Optimized	1.4 - 2.8	Allowable pressure range in mass models
Recuperator dP/P (%)	Optimized	0.5% - 4%	Assumed range of possible mass optimized designs
Reactor dP/P (%)	Model based	Model based	Calculated as a result of inlet conditions and desired outlet temperature
Recuperator effectiveness (%)	Optimized	72% - 94%	Assumed range of possible mass optimized designs

B. Mass Model

The mass of the power system is estimated from a buildup of component-level mass models. These component-level mass models are based on a combination of first principles physics-based scaling, published relations, and point designs scaled up and down in power. These models were originally published in Ref. [7], and several are updated in the present work. The heat exchanger mass models are now based on a first principles model of a basic heat exchanger design with correlations used to scale this design based on state points from the performance model. The detailed description of one of these designs, the heat pipe heat exchanger, is described by Nikitaev in Ref. [8]. In addition, improved geometery assumptions were added to the reactor mass model, and the PMAD mass model is composed of component-level parametric mass estimates based on relations developed by Metcalf in Ref. [9].

The mass model is integrated with the performance model and used to calculate the masses of each component from outputs of the performance model, such as mass flow rate, radiator area, and reactor power. The mass model is parametric and can handle a wide range of inputs. When involved in the optimization routine in section A.1, particular variables such as the compressor inlet temperature (CIT) can be optimized such that α_{PS} is minimized.

III. Reference Cases

A. Reference cases for 1200K and 1400K

Specific performance model cases were selected as a reference around which the sensitivity and Monte Carlo analyses were performed. These cases are the result of optimizing the cycle for minimum α_{PS}. Assumptions for the model inputs that were not part of the optimization process were selected based on literature review, subject matter expert recommendations, and trends within the physics-based mass models. A NEP system layout of four Brayton units, one reactor, and one radiator was selected with a total electrical power output of 2 MW_e. The working fluid of all four Brayton units was assumed to mix and enter the reactor core without additional losses. The resulting values for the optimized inputs for the 1200K and 1400K power conversion inlet temperatures (PCIT) are shown in Table 2. Power cycle diagrams with key metrics and operating states are displayed in Figure 3 and Figure 4. The breakdown of component level α values for the two reference cases are shown in Figure 5.

Table 2. Optimized variable values and results

Variable	Optimized Value at 1200K PCIT	Optimized Value at 1400K PCIT
Power Conversion Inlet pressure (MPa)	2.1	2.1
CIT (K)	357	378
Turbine PR	2.37	2.70
Recuperator dP/P (%)	0.58	0.65
Recuperator effectiveness (%)	94	94
Cycle efficiency (%)	33.7	36.8

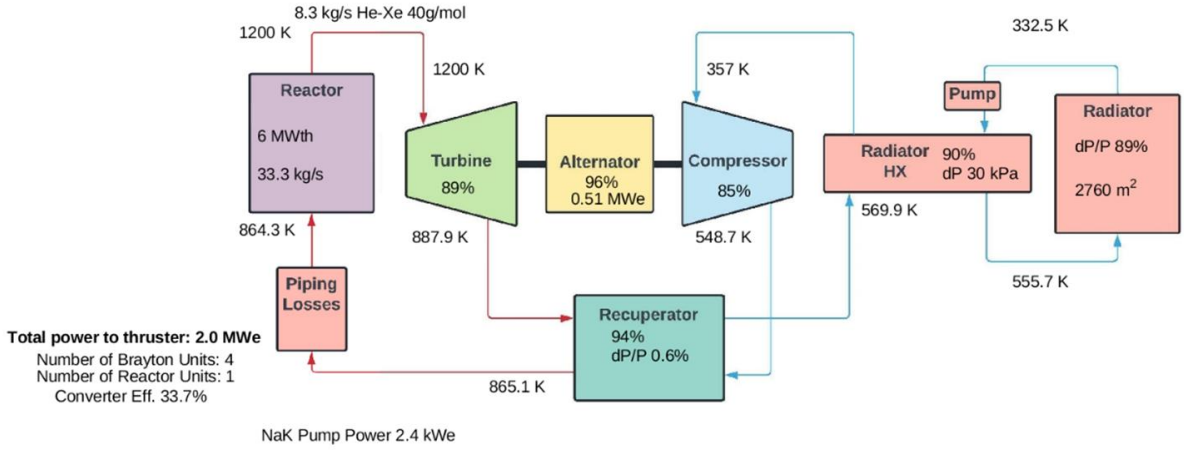

Figure 3. Reference power cycle diagram for 1200K PCIT

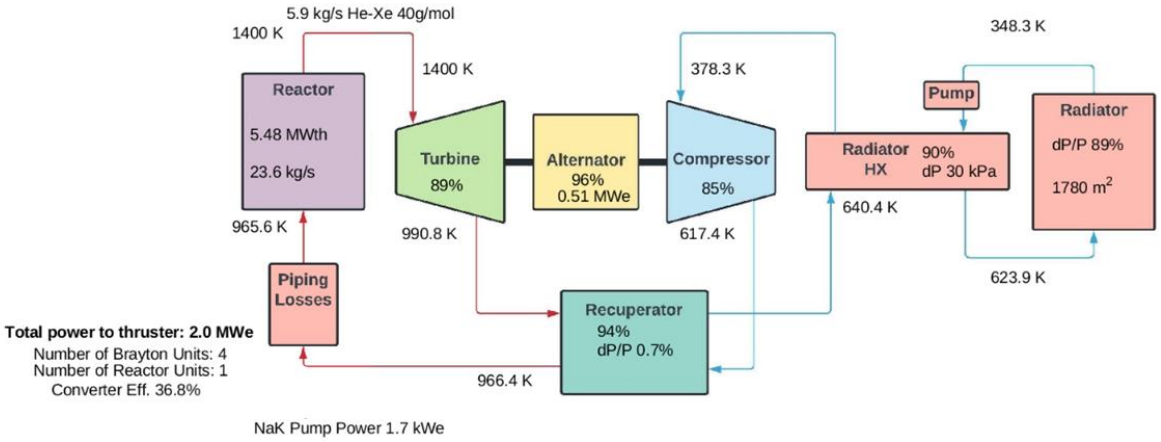

Figure 4. Reference power cycle diagram for 1400K PCIT

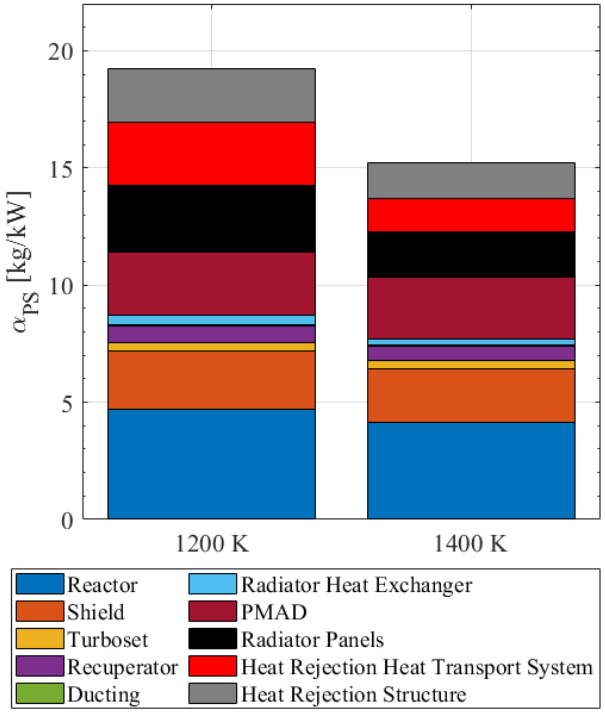

Figure 5. Breakdown of α_{PS} by major assembly (2 MW_e power, gas-cooled reactor) for PCIT of 1200 K and 1400 K)

Both reference cases optimized to the lower limit of the power conversion inlet pressure. Analysis shows that the lower mass at lower pressure is a result of thinner ducting and pressure vessel walls, which offsets the efficiency and pressure loss improvements that could be realized in a higher pressure system that would have heavier duct walls. The CIT is optimized to a value that primarily balances the effects of system efficiency and average radiator temperature on overall mass. Decreasing the CIT allows for a higher cycle efficiency and therefore lower system mass flow rate, which reduces reactor mass and average radiator areal density through a commensurate reduction in ducting requirements. A colder CIT also means the radiator will be cooler and reject less waste heat per area, requiring a larger radiator area. An intermediate temperature balances these two competing effects. The recuperator optimizes to a high effectiveness and low pressure drop despite the high mass of this combination. The recuperator has a large impact on the cycle efficiency and temperatures within the system so the mass increase of the recuperator has a net benefit in reduced masses for other larger components. The sensitivity of the recuperator parameters is further explored in the sensitivity analysis section.

B. Additional Considerations

In these reference cases α_{PS} is minimized, but future work could consider minimizing radiator area so it would either fit in a launch vehicle or reduce the amount of in-space assembly required. Preliminary reference cases that optimized for minimum radiator area have been created. These cases had much higher turbine inlet pressures of 4.8 MPa, a CIT of 490K, and a lower turbine pressure ratio. This reduced the radiator area from 2760 m^2 to 2376 m^2 while increasing the α_{PS} from 19 kg/kW_e to 28 kg/kW_e. The efficiency of the system decreased from 33.7% to 20.1% due to the higher CIT. The high CIT resulted in higher radiator temperatures and greater power throughput per unit area of radiator, yielding a reduced radiator area despite it being a less efficient power conversion cycle. From these simple reference cases we find that both α_{PS} and radiator area will need to be considered in the development of an NEP system.

Reference cases with an alternative configuration of the Brayton cycle, where the reactor utilized heat pipes in the core and was on a separate fluid loop, were also created. These cycles displayed similar sensitivity trends and had benefits such as flexibility in the reactor working fluid selection and adjustable temperature drop across the core. The additional components did generally result in a higher α_{PS}. Analysis and comparison of these configurations are left for future work.

IV. Sources of Uncertainty

A. Performance Assumption Uncertainty

Because of the uncertainty in future technology development and detailed component design, the parameters used in the Brayton cycle are given values that indicate the range between the current capabilities of the technology and potential future capabilities assuming aggressive and successful technology development. A Monte-Carlo analysis that incorporates this range of potential values can be used to determine the confidence level that KPPs can be met, and how specific technology development could improve this confidence.

The range of values chosen for the Monte Carlo analysis are detailed in Table 3. The minimum values are meant to represent what current technology can conservatively produce, while the nominal values are the expected performance assuming reasonable technology development. The maximum values are generally the maximum realistic values found in the literature. A triangular distribution was chosen to capture the most likely probability of the nominal value and tapering off to the minimum and maximum values.

Table 3. Performance model variable uncertainty range

Parameter	Min	Nominal	Max	Comment
Turbine isentropic efficiency (%)	85	89	93	Lower bounds set by prototype capabilities (Sandia C30, BRU, etc) and higher bounds set by CFD and helium power plant studies [10], [11], [5]
Compressor isentropic efficiency (%)	80	85	91	Lower bounds set by prototype capabilities (Sandia C30, BRU, etc) and higher bounds set by CFD and helium power plant studies [10], [11], [5]
Recuperator effectiveness	80	85	94	Preliminary mass optimized design range
Recuperator dP/P (%)	0.5	1	4	Preliminary mass optimized design range
Radiator HX dP/P (Brayton side) (kPa)	10	30	50	Preliminary mass optimized design range
Radiator HX effectiveness (%)	80	90	90	Lower bound from CBC fission surface power study, upper bound set by AMA modeling results [12]
Radiator Emissivity	0.8	0.9	0.9	Bounds set by ISS radiator capability and common materials [13]
Radiator Sink Temp (K)	4	4	10	Deep space temperature with margin
Liquid Metal Pump efficiency (%)	40	44	65	NaK pump based on SNAP-8 and additional studies [14]
Alternator efficiency (%)	92	96	98	Literature review of CBC in-space application hardware [5]

B. Mass Model Uncertainty

Some inputs to the mass model were also identified to be of interest in the Monte-Carlo simulation. The ranges for these values come from subject matter experts and engineering judgment and are listed in Table 4. The ranges in values represent estimated uncertainties in the mass model results, given a set of technology selections. In addition to

the uncertainty in the mass model inputs, there is significant uncertainty in the component mass estimates themselves, stemming from low maturity of the subject technologies and simplifications needed so the model could be solved rapidly over a wide trade space. The estimated uncertainty for major components (Table 5) is based on each component model's estimated accuracy and the maturity of the underlying technology. From this table it can be observed that some of the components have higher uncertainty at the higher 1400 K PCIT reference case since the materials needed to achieve higher temperatures are not as mature. Other important sources of uncertainty include the use of optimistic scaling equations and correlations, additional margin on the radiator area required to account planetary albedo or less effective heat transfer in heat pipes and panels, relatively simplistic mass models that scale with area for items such as the radiator structure, and generally low maturities of the components.

Table 4. Mass model variable uncertainty range

Parameter	Min	Nominal	Max	Comment
Liquid metal pump specific power (kg/kW)	0.13	0.26	0.4	Significant uncertainty around pump specific mass [9]
Parasitic load radiator high temperature (K)	925	925	1225	Depending on heat pipe /radiator could go significantly higher, no benefit to going colder
Alternator voltage (V)	750	1000	1250	No reason to bias one way or the other [9]
Alternator frequency (kHz)	2.4	3	3	Lower mass at higher frequencies, frequency limited by shaft rotational velocity, 3 kHz is at the high end [9]
Thruster voltage (V)	300	400	500	No reason to bias one way or the other [9]
Width of radiator panel module (m)	0.65	1.29	1.935	No reason to bias one way or the other [7]

Table 5. Estimated Uncertainty in Major Components Mass Estimates

Component	1200 K PCIT	1400 K PCIT	Comments
Heat Rejection Structure	-20% to 30%	-20% to 30%	Simple scaling with radiator area results in some symmetric uncertainty, additional uncertainty from larger required area
Radiator Panels	-10% to 15%	-10% to 15%	Uncertainty in heat pipe spacing and panel thickness is symmetrical, additional uncertainty from larger required area
Heat Rejection Heat Transport System	-25% to 25%	-25% to 25%	Uncertainty depends on ducting layout
PMAD	-10% to 10%	-10% to 10%	Uncertainty bias unknown
Turboset	-20% to 15%	-30% to 20%	Bias to lower mass since turbine and compressor were assumed to be reasonable
Recuperator	-13% to 20%	-13% to 20%	Based on testing with first principles model
Ducting	-20% to 20%	-20% to 20%	No reason to bias one way or the other
Reactor	-10% to 10%	-20% to 20%	Pressure vessel scaling is very conservative, but other components will be more likely to be heavier
Shield	-5% to 10%	-10% to 20%	
Radiator Heat Exchanger	-50% to 50%	-50% to 50%	Based on testing with first principles model
Reactor Heat Exchanger	-5% to 100%	-5% to 100%	Based on testing with first principles model

V. Perturbation of Variables

A. Sensitivity of inputs

In the analyses performed for this study, the method for sensitivity evaluation is as follows:

1. Calculate reference case for the point of minimum α_{PS} for a given set of assumptions.
2. Calculate partial derivatives of parameters with respect to α_{PS} at the reference points by perturbing the parameter within the model precision limitations.

The results of this process are shown in Figure 6. The major drivers are:

- An improvement of 1% in the turbine or compressor efficiency results in a 2% reduction in α_{PS} at the optimization point for both 1200K and 1400K PCIT reference cases.
- An improvement of 1% in the radiator heat exchanger effectiveness results in a 2% reduction in α_{PS} due to its direct effect on the radiator temperature and therefore average radiator temperature
- α_{PS} is minimally sensitive to variations in the recuperator effectiveness and CIT because there is a small gradient in α_{PS} with respect to these variables in the neighborhood of the minimum α_{PS} solution
- An increase of 1% in the recuperator pressure drop increases the α_{PS} by 2%. This pressure drop affects the working fluid twice in the cycle over a large temperature range, and the recuperator mass behaves exponentially at the optimized point of low pressure drop and high effectiveness. The combination of these effects results in the α_{PS} being sensitive to the recuperator pressure drop.
- α_{PS} is relatively insensitive to variations of 100 kPa in the turbine inlet pressure

After examining all the sensitivity of α_{PS} to variations in the performance for all components, we find that by far the greatest sensitivity is relative to variation in the PCIT. At a reactor temperature of 1200 K, an increase in PCIT of 50 K results in a decrease in α_{PS} of 9% relative to the reference case, while for a 1400 K reactor the value of α_{PS} only decreases by 3.5%, indicating potential diminishing returns for further increases in PCIT.

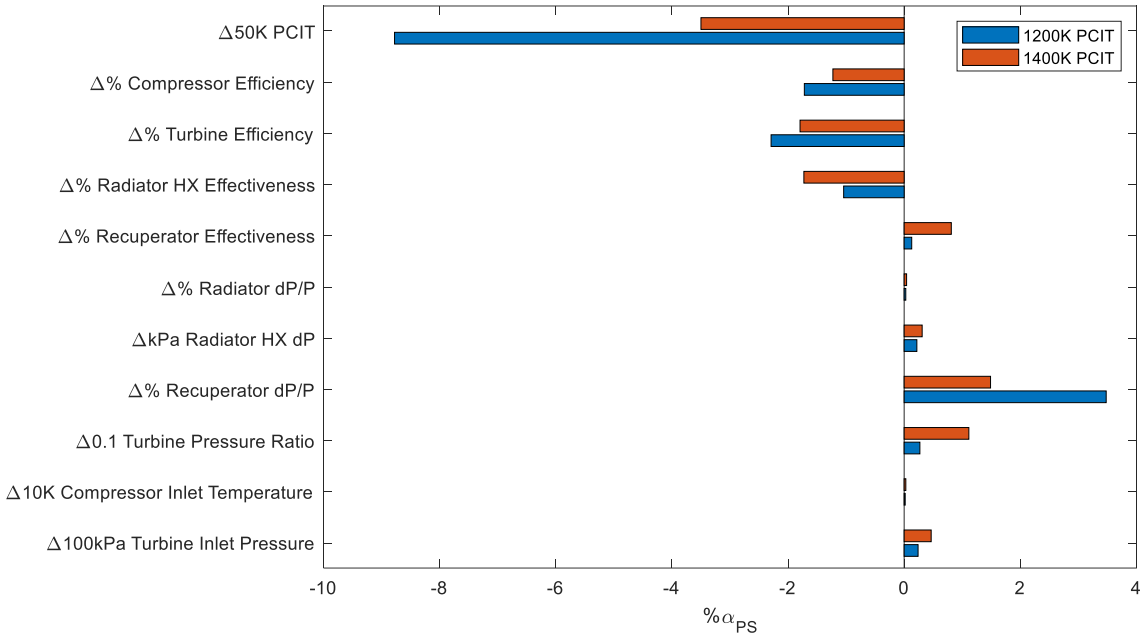

Figure 6. Sensitivity analysis of select variables

B. Sensitivity to CIT and PCIT

Additional figures that show the functional relationship in the optimized α_{PS} relative to variations in CIT or PCIT are shown in Figure 7 and Figure 8. The CIT has an exponential impact on α_{PS} as the temperature is decreased from the minimum point. This is driven by the radiator area increasing to compensate for a reduction in radiative heat transfer per unit area, as the latter is greatly reduced at lower radiator temperature due to the T^4 scaling of radiation. Increasing the CIT above the minimum shows a more linear trend as the mass increases gradually as the system efficiency decreases. A difference of 4 kg/kW$_e$ is shown when increasing the CIT from the minimum value to 100K higher than minimum.

The PCIT has a logarithmic trend with α_{PS} due to the benefits decreasing as the temperature rises. Increasing the PCIT from 1150K to 1200K decreases α_{PS} by 1.7 kg/kW$_e$. With respect to all the variables considered in the sensitivity analysis the PCIT and CIT have the largest relative impact on α_{PS} at 1200K PCIT.

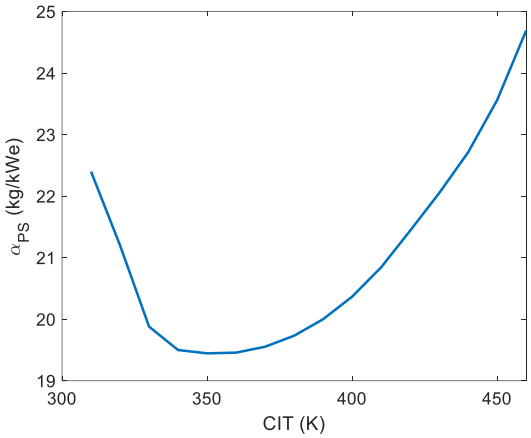

Figure 7. CIT and α_{PS} (gas -cooled Reactor with PCIT of 1200 K)

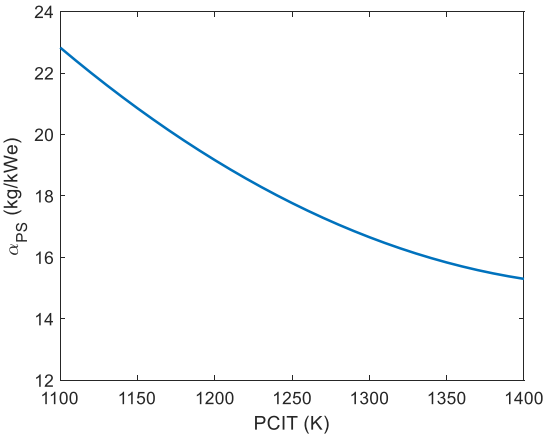

Figure 8. PCIT and α_{PS} (gas -cooled Reactor)

VI. Monte Carlo Analysis

To assess uncertainty in α_{PS} as a result of uncertainties in performance inputs and mass estimates, a Monte Carlo simulation was performed using the ranges and probability distributions in Table 3 through Table 5. For each trial, the inputs were re-optimized to minimize α_{PS}. For the results below, the PCIT is held constant at 1200 K; therefore, the histograms represent the uncertainty in component performance and mass for a system targeting 1200K PCIT with four Brayton units, one reactor, and one radiator at an electrical power level of 2 MW_e. A simulation of 200 trials results in the histograms in Figure 9 through Figure 11.

The mean value and the reference case α_{PS} value is labeled. A log-normal distribution curve is overlayed onto the histogram. The α_{PS} plot showed a 90% confidence interval of 18 to 23 kg/kW_e with the reference value representing a possible α_{PS} if the technology development goals are met. The radiator area had a 90% confidence interval of 2300 to 3500 m^2. The cycle efficiency, defined as the produced electrical power from the PMAD over the reactor thermal power, had a 90% confidence interval of 31% to 36%. The confidence interval of the data demonstrates the probability of likelihood that the α_{PS} value will fall within the bounds. Feeding this information into a higher level mission analysis can provide an initial estimate of the potential impact of development uncertainty on total vehicle mass and launch vehicle selection.

An additional Monte-Carlo simulation was completed without the model re-optimizing at each trial, resulting in in off-nominal designs centered around the reference case. This could represent a scenario where certain design choices of the power conversion system are fixed early in the development process and cannot be adjusted later as component designs are finalized. The histogram and log-normal distribution is shown in Figure 12. Compared to the optimized Monte-Carlo simulation the mean α_{PS} increases by approximately 1.5 kg/kW_e, and the 90% confidence interval widens.

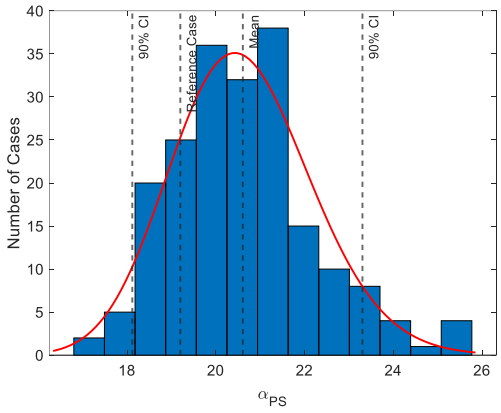

Figure 9. Histogram and probability distribution of α_{PS}

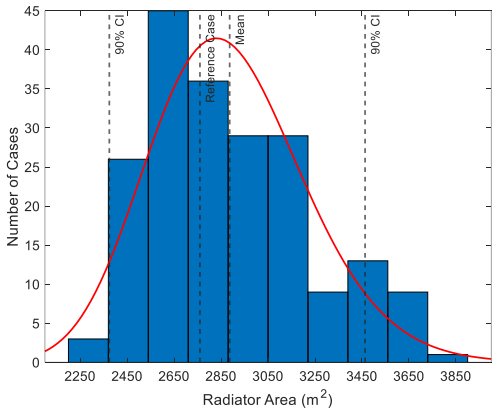

Figure 10. Histogram and probability distribution of radiator area

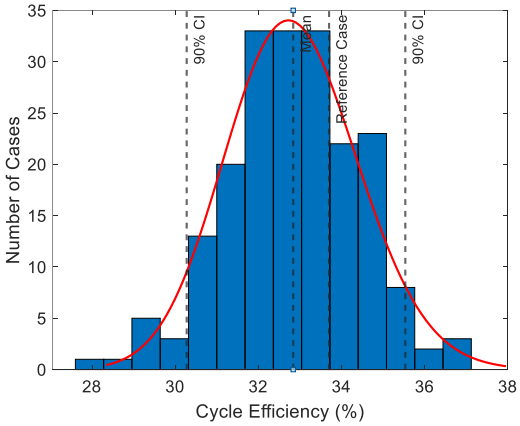

Figure 11. Histogram and probability distribution of cycle efficiency

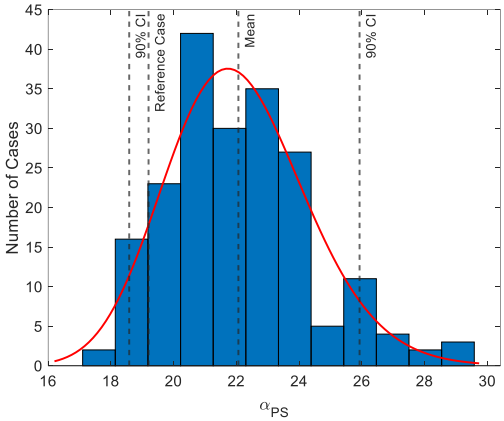

Figure 12. Histogram and probability distribution of unoptimized α_{PS}

These results give information on the uncertainty in α_{PS}, but are limited in that they do not encompass the full range of possible PCIT values. NASA SNP plans to target development of a system with PCIT up to 1400 K. As shown in Figure 5, this would result in significantly lower alpha. When a uniform probability distribution is applied to PCIT as an additional input, and the optimized and non-optimized results are mixed to include additional uncertainty, a new distribution can be generated. This distribution spans the optimistic end of 1400K PCIT optimized through 1200K PCIT unoptimized. Figure 13 shows the results of this analysis, where 70% of cases are optimized. This wider distribution has a mean of 18.5 kg/kWe, a 90% confidence interval of 15.5 to 21.9 and represents the fullest picture of development result uncertainty that we can currently predict. As development progresses, and as subject matter experts provide input to improve the input variable probability distributions, the picture of expected uncertainty will evolve and update to the project's best understanding.

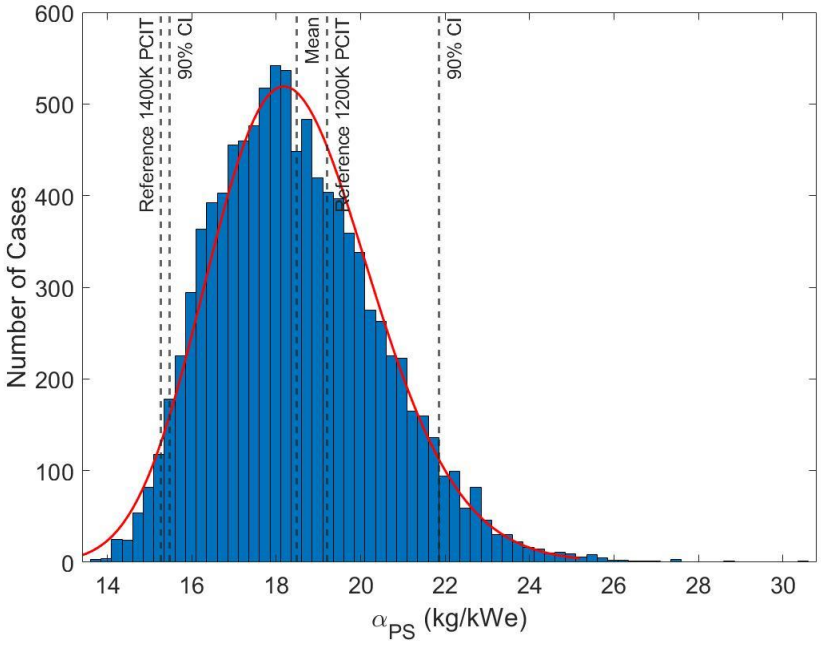

Figure 13. Histogram and probability of α_{PS} for PCIT 1200K-1400K, 10000 cases with 70% optimized

VII. Case Studies

A. Component Mass Sensitivities

In addition to sensitivity and uncertainty analysis, the integrated performance and mass models can be used to analyze specific cases of interest, such as if the technology development effort fails to produce components at the expected mass threshold. Two examples of this include the recuperator being three times more massive than predicted by the mass model and the heat rejection system being 30% larger in mass than predicted. These cases were chosen due to their high degree of interrelation with the rest of the system; the way in which these two systems are optimized has a large effect on the cycle performance as a whole. For each case, the system will be re-optimized to find the minimum α_{PS} after the component masses have been adjusted. Figure 14 shows how the α of the CTEs changes when the recuperator and radiator are assumed to be 300% and 30% larger, respectively. When the recuperator mass is tripled, the system optimizes to have a much less effective recuperator, since the mass of the recuperator is strongly correlated with its effectiveness. The reduction of effectiveness results in a recuperator of approximately the same mass as the reference case. The α increase comes from the PHRS where the reduced recuperator effectiveness reduces cycle efficiency and CIT which therefore increases the required radiator area. For the second case, the result is a straightforward increase in heat rejection mass, with little meaningful change in the optimization of the system. These same trends also hold true for varying PCIT and system configurations.

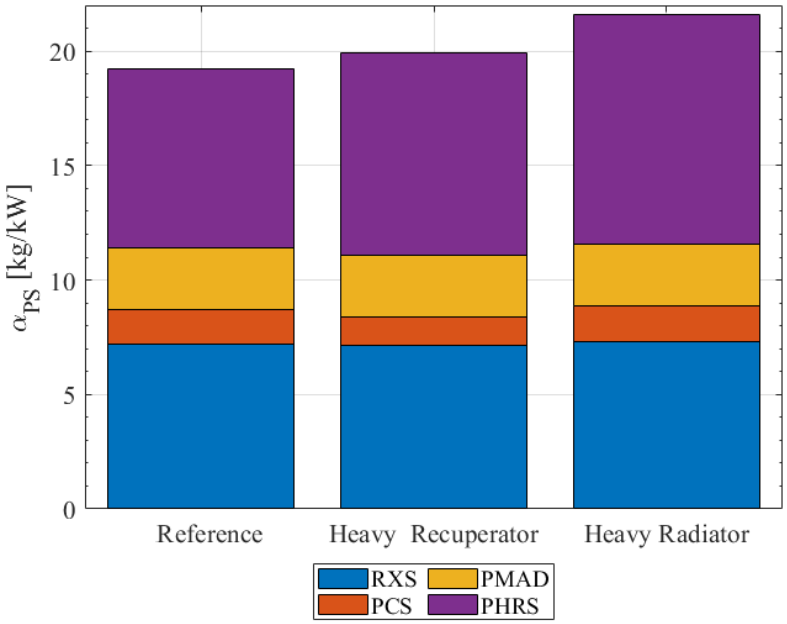

Figure 14. Mass sensitivity case studies (gas-cooled reactor with PCIT of 1200 K)

B. Reactor ΔT Limitations

The sensitivity analysis discussed above are optimized by minimizing α_{PS}, however, other requirements may constrain the practical operating limits of the Brayton cycle. For example, current work on the reactor technology development indicates that due to material limitations, a lower reactor ΔT will be important in lowering the reactor development risks. The system can be re-optimized to meet these requirements, but the cost of doing so will result in a higher α_{PS}. When minimizing the reactor ΔT, some engineering judgment must be applied to what a realistic minimum should be. Figure 15 shows how efficiency drastically decreases when the reactor ΔT is reduced; a point must be selected that can reduce the reactor ΔT without resulting in a system with an efficiency that is too low. The reason for this effect is that as the reactor ΔT is decreased, the mass flow rate must be increased to transfer the same amount of energy. This in turn reduces the efficiency of the cycle and increase the CIT. There are diminishing returns to decreasing the reactor ΔT, as at lower efficiencies the reactor output power must be larger causing the ΔT to increase again losing most of the initial change in ΔT. Figure 15 shows that the cost in α_{PS} when going to this lower ΔT cycle is 3.4 kg/kW$_e$.

The minimum ΔT that can be achieved in the reactor is approximately 200 K for the 1200 K PCIT case and 250 K for the 1400 K PCIT case. If material limitations require a lower ΔT in the reactor, additional heat exchangers may be used to interface the reactor with the rest of the NEP system and doing this may increase α_{PS}.

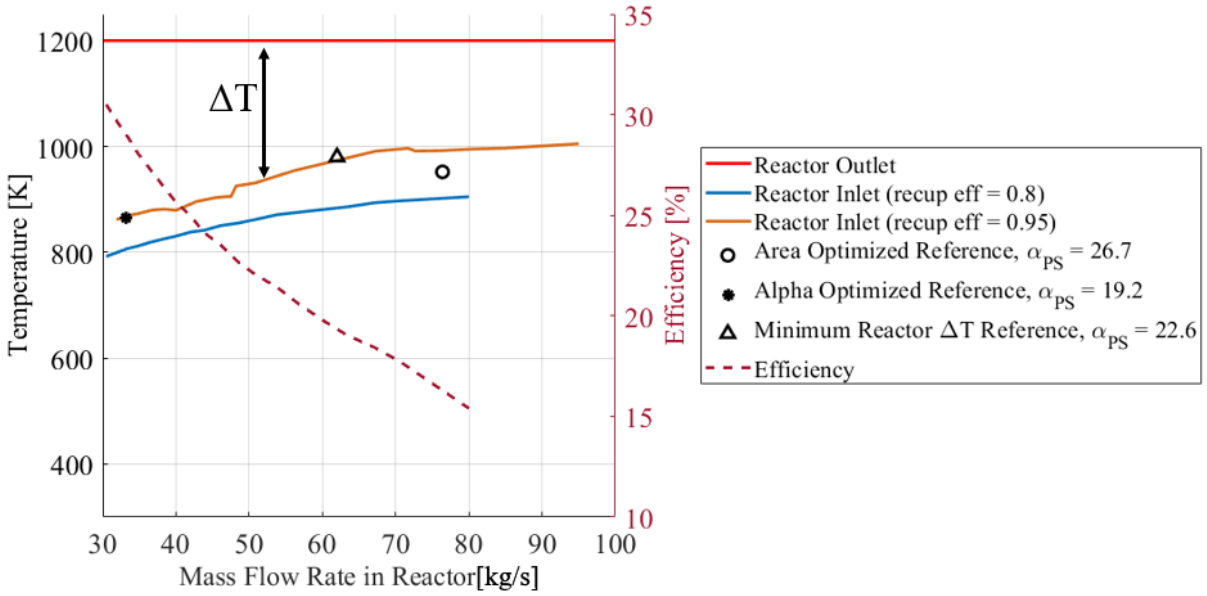

Figure 15. Reactor ΔT limitations (gas-cooled reactor with PCIT of 1200 K)

VIII. Conclusions

In support of NASA's space nuclear program, a MW-class NEP system was examined with sensitivity and Monte-Carlo analyses. Power conversion performance and mass modeling was used to optimize a system with a gas-cooled reactor towards minimum mass, with a general trend towards lower system pressures, high recuperator performance, and a CIT under 370K that result in a system efficiency of at least 33%. The sensitivity analysis identified that the PCIT had the greatest impact on system mass, and temperature increases of 50K could decrease α_{PS} by as much as 2 kg/kW$_e$ for a 2MW$_e$ configuration. Operating the cycle at the optimal CIT also had an impactful effect on α_{PS}. Assessing the uncertainty in α_{PS} due to the modeling parameters was done by a Monte-Carlo analysis which quantified the variance in possible α_{PS}. The reference cases had lower α_{PS} compared to the mean of the analysis, with a 90% confidence interval spanning approximately 5 kg/kW$_e$. Case studies were also performed to see the direct effect of certain scenarios, including a much higher recuperator and radiator mass as well as reactor temperature drop limitations. Future work may investigate the comparison between gas cooled and heat pipe reactor configurations, and include additional uncertainty analyses. The analyses described in this paper can inform recommendations towards the most beneficial technology development, KPP selections, and human Mars mission design.

IX. Acknowledgements

This work was supported by NASA's Space Technology Mission Directorate (STMD) through the Space Nuclear Propulsion (SNP) project. This work was funded under Contract No. 80LARC17C0003.

X. References

[1] K. A. Polzin, A. K. Martin, F. M. Curran, R. M. Myers and M. A. Rodriguez, "Strategy for Developing Technologies for Megawatt-class Nuclear Electric Propulsion Systems," in *IEPC*, Boston, 2022.

[2] M. Duchek, W. Machemer, C. Harnack, M. Clark, A. Pensado and K. Palomares, "Key Performance Parameters for MW-Class NEP Elements and Their Interfaces," in *AIAA ASCEND*, Las Vegas, 2022.

[3] R. Dyson, D. V. Rao, M. Duchek, C. Harnack, R. Scheidegger, L. Mason, A. Juhasz, L. Rodriguez, R. Leibach, S. Geng and D. Goodell, "Nuclear Electric Propulsion Brayton Power Conversion Working Fluid Considerations," in *NETS*, Cleveland, 2022.

[4] C. Harnack, W. Machemer, M. Duchek, E. Grella, D. Nikitaev and C. Smith, "Brayton Cycle Power Conversion Model for MW-Class Nuclear Electric Propulsion," in *Nuclear and Emerging Technologies for Space*, Cleveland, 2021.

[5] L. S. Mason and J. G. Schreiber, "A Historical Review of Brayton and Stirling Power Conversion Technologies for Space Applications," in *Space Nuclear Conference*, 2007.

[6] K. Polzin, R. Dasari, R. Myers, J. Kesseli, J. Breedlove and J. Laube, Interviewees, *NEP Technology Roundtable Discussion*. [Interview]. 27 8 2021.

[7] W. Machemer, M. Duchek, C. Harnack, E. Grella, D. Nikitaev and C. Smith, "Mass Modeling of NEP Power Conversion Concepts for Human Mars Exploration," in *Nuclear and Emerging Technologies for Space*, Cleveland, 2022.

[8] D. Nikitaev, "Heat Pipe Heat Exchanger for Nuclear Electric Propulsion Power Conversion System," in *AIAA ASCEND*, Las Vegas, 2022.

[9] K. J. Metcalf, "Power Management and Distribution (PMAD)," National Aeronautics and Space Administration CR 217268, Cleveland, Model Development.

[10] E. Staff, "Brayton Isotope Power System Phase 1 First Annual Report," Airesearch Manufacturing Company, Phoenix, 1976.

[11] S. A. Wright, R. J. Lipinski, M. E. Vernon and T. Sanchez, "Closed Brayton Cycle Power Conversion Systems for Nuclear Reactors: Modeling, Operations, and Validation," Sandia National Laboratories, Albuquerque, 2006.

[12] R. L. Fuller, "Closed Brayton Cycle Power Conversion Unit for Fission Surface Power Phase I Final Report," NASA, Cleveland, 2010.

[13] G. Tuan, D. Westheimer, G. Birur, D. Beach, D. Jaworske, W. Peters and J. Triolo, "Evaluation of Coatings and Materials for Future Radiators," in *ICES*, Norfolk, 2006.

[14] K. A. Polzin, "Liquid-Metal Pump Technologies for Nuclear Surface Power," NASA, Marshall Space Flight Center, 2007.

[15] S. Oleson, L. Burke, L. Mason, E. Turnbull and S. McCarty, "Compass Final Report: Nuclear Electric Propulsion (NEP)-Chemical Vehicle 1.2," NASA Glenn Research Center, Cleveland, 2021.

[16] S. A. Wright, "Summary of the Sandia Supercritical CO2 Development Program," Sandia National Laboratories, Albuquerque, 2011.

[17] T. Neises and C. Turchi, "A comparison of supercritical carbon dioxide power cycle configurations with an emphasis on CSP applications," *Energy Procedia*, vol. 49, pp. 1187-1196, 2014.

[18] S. Khandelwal, C. Hah and L. M. Powers, "Fabrication Materials for a Closed Cycle Brayton Turbine Wheel," NASA, Glenn Research Center, 2006.

[19] M. S. El-Genk, J.-M. P. Tournier and B. M. Gallo, "Dynamic Simulation of a Space Reactor System with Closed Brayton Cycle Loops," *Journal of Propulsion and Power*, vol. 26, no. 3, pp. 394-406, 2010.

[20] D. G. Gilmore, Spacecraft Thermal Control Handbook, El Segundo: AIAA, 2002.